Eur. Phys. J. B **9**, 187–199 (1999)

THE EUROPEAN PHYSICAL JOURNAL B

EDP Sciences

Quantum theory of the magneto-optical effect induced by Ni^{2+} ions in barium ferrites

X. Zhang[1], Y. Xu[2], and M. Guillot[3,a]

[1] Department of Physics, Nanjing University, Nanjing 210008, and Department of Physics, Teacher's College, Yangzhou University, Yangzhou 225002, P.R. China
[2] CCAST (World Laboratory), PO Box 8730, Beijing 100080, and Department of Physics, Nanjing University, Nanjing 210008, and National Key Laboratory of Magnetism, Institute of Physics, Chinese Academy of Sciences, Beijing 100080, P.R. China
[3] Laboratoire des Champs Magnétiques Intenses, CNRS/MPI, B.P. 166, 38042 Grenoble Cedex 9, France

Received 7 January 1998

Abstract. To reveal the physical origin of the giant magneto-optical enhancement of Ni^{2+} ions in barium ferrite, quantitative calculations of the contributions of both the intra-ionic electric dipole transition between the $3d^8$ and $3d^7 4p$ configurations of the Ni^{2+} ions and the intra-ionic electric dipole $d \rightarrow d$ transition induced by odd-parity crystal field terms are presented. It is deduced that the $3d^8 \rightarrow 3d^7 4p$ transition is important in the origin of the considered magneto-optical enhancement. The most important factor is the Ni-Fe superexchange interaction; since it is strong enough, the Faraday rotation produced by the Ni^{2+} ions is large though the energy difference between the $3d^8$ and $3d^7 4p$ configurations is large. It is demonstrated that though the intra-ionic electric dipole $d \rightarrow d$ transition does produce Faraday rotation peaks in the visible range, their magnitude is too small to explain the observed Faraday rotation. The effect of the spin-orbit interaction on the Faraday rotation is analysed. The spin-orbit interaction of the ground configuration plays a very important role in the occurrence of Faraday effects, but the Faraday rotation does not increase linearly with the strength of the spin-orbit coupling. On the contrary, the spin-orbit interaction of the excited configuration has almost no effect on the Faraday rotation. It is shown that the mixing of the different multiplets of the ground term induced by the crystal field has a great influence on the magneto-optical properties.

PACS. 78.20.Ls Magnetooptical effects – 75.50.Gg Ferrimagnetics

1 Introduction

Following a long period of development, first generation optical data storage systems using erasable magneto-optical (MO) materials based on the rare-earth transition-metal alloys are now available. These materials used in the visible range have been tailored with respect to their MO and magnetic properties. However, some properties of these materials are still less than satisfactory. With new techniques developed to prepare garnets and ferrite thin films [1–4], magnetic oxides again become potential candidates for the MO recording material. While oxide thin films are able to overcome some of the major deficiencies of the rare-earth transition-metal alloy films, some properties of these materials, *e.g.*, the uniaxial anisotropy, the coercivity, the grain size, and the high crystallization temperature, require further improvement for the MO recording application. The barium ferrite has a marked uniaxial anisotropy and good squareness of the in-plane hysteresis loop but the MO response remains quite poor. It is known that the MO effects in ferrites may be substantially enhanced by ion substitution. In barium ferrite, substitution using Co^{2+} ions has already been the subject of many reports [5–8]. Recently, it was found that Ni substitution in barium ferrites enhances strongly the Kerr and Faraday rotations [9,10]. Gomi *et al.* reported that the enhancement factor of specific Faraday rotation at 496 nm wavelength (2.5 eV photon energy) is as large as 20 000 degr cm^{-1}/x for $Ba_{1-x}M_xFe_{12-x}Ni_xO_{19}$ films prepared by sputtering, where M is La or Pr which is substituted for Ba^{2+} ions for charge compensation and has no contribution to the Faraday rotation [9]. Consequently, Ni-substituted barium ferrite becomes a potential candidate for the MO recording material.

Theoretical investigations that support the effort to achieve high quality MO recording material based on the magnetic oxides of $3d$ elements are, however, scarce. To our knowledge, only some qualitative explanations for the origin of the MO enhancement of Co substitution in ferrites have been given [11–13]. The following two models have been suggested: the intra-ionic $d \rightarrow d$ electric dipole transitions and the charge-transfer transitions. It is

[a] e-mail: mguillot@labs.polycnrs-gre.fr

well-known that the pure $d \rightarrow d$ electric dipole transitions are forbidden by the Laporte's rule. However, the Co^{2+} ions in some ferrites occupy crystal sites which have no center of symmetry. Then the odd-parity crystal field (CF) potential terms mix the $4p$ orbitals of the Co^{2+} ions with the $3d$ orbitals in the same ion, and consequently the crystal-field split $3d$ levels contain small $4p$ components. In general, the $4p$ components contained in the low-lying crystal-field split $3d$ levels are very small, while those in the higher-lying $3d$ levels may be not negligible and lead to the so called intra-ionic $d \rightarrow d$ electric-dipole transition probability [11–13]. Furthermore, in the case of transition metal complexes the selection rules are relaxed by vibronic interaction [13]. This also leads to $d \rightarrow d$ electric-dipole transitions. About the charge-transfer transition, we note that because of the covalent and superposition effects the excited states of the Co ion may be hybridized with ligands' states and, as a result, bonding and antibonding levels are created. The relative weights of the Co states and ligands' states in the bonding levels are different from those in the antibonding levels. Therefore the electric dipole transitions between the bonding and antibonding levels involve charge transfer between the Co ions and their ligands.

Before our work, for the $3d$ ions, the possibility of inducing large MO effects by the intra-ionic $3d^n \rightarrow 3d^{n-1}4p$ electric dipole transitions has never been considered. We have shown theoretically that the intra-ionic $4f^n \rightarrow 4f^{n-1}5d$ electric dipole transition is the main origin of the giant MO enhancement of rare earth ions in some compounds [14–16]. Since the energy difference between the $3d^n$ and $3d^{n-1}4p$ configurations in the $3d$ ions is much larger than that between the $4f^n$ and $4f^{n-1}5d$ configurations in the rare earth ions, for $3d$ ions, the factor $\omega^2/(\omega_{ng}^2 - \omega^2)$ (see Eq. (4)) is small in the visible and infrared bands. So, after a first consideration it seems that the intra-ionic $3d^8 \rightarrow 3d^7 4p$ electric dipole transitions cannot produce a large Faraday effect. To conciliate this conclusion with the experimental data given above, the spontaneous Faraday rotation caused by the intra-ionic $3d^n \rightarrow 3d^{n-1}4p$ electric dipole transitions in the Ni^{2+} ions in the barium ferrite is calculated and the results are compared with the observed data (Sect. 2). According to the high value of the Neel temperature, the superexchange interaction acting on the Ni^{2+} ions in the barium ferrite is much larger than that on the rare-earth ions in iron garnets and it will be shown that the large superexchange interaction leads to a very large Faraday rotation in the Ni-substituted barium ferrite though, for the Ni^{2+} ions, the frequency factor $\omega^2/(\omega_{ng}^2 - \omega^2)$ is small. Because there is still no quantitative analysis of the Faraday rotation produced by the $d \rightarrow d$ electric dipole transitions, the contribution of the intra-ionic dipole $d \rightarrow d$ transitions of the Ni^{2+} ions at the barium ferrite induced by the odd-parity crystal field to the Faraday rotation is studied quantitatively in Section 3. The role of the spin-orbit interaction in the MO phenomena is a very interesting problem, it is analysed in Section 4. Finally, the conclusions to be drawn from this work are given in Section 5.

2 Intra-ionic 3d → 4p electric dipole transition

At a macroscopic scale, the propagation of electromagnetic waves is described by the electric and magnetic permeabilities ε and μ. For a crystal with at least threefold symmetry to the z axis and a magnetization parallel to this axis, the dielectric tensor has the form

$$\varepsilon = \begin{pmatrix} \varepsilon_{xx} & \varepsilon_{xy} & 0 \\ -\varepsilon_{xy} & \varepsilon_{xx} & 0 \\ 0 & 0 & \varepsilon_{zz} \end{pmatrix} \tag{1}$$

all elements of which are complex and can be expressed as

$$\varepsilon_i = \varepsilon_i' + j\varepsilon_i''. \tag{2}$$

The diagonal element ε_{xx} is related to the normal refractive index n and the normal extinction coefficient k. The off-diagonal element ε_{xy} is related to the differences of the refractive indices $n_\pm$ and of the extinction coefficients $k_\pm$ of right and left circularly polarized light [17].

When the optical absorption is weak, the specific Faraday rotation caused by the electric dipole transitions is known to be given by [17,18]

$$\theta_{\mathrm{F}} = \frac{1}{9}(\bar{n}^2 + 2)^2 \frac{\pi}{\lambda \bar{n}} \varepsilon_{xy}'', \tag{3}$$

here the Lorentz-Lorenz correction factor has been included. $\bar{n}$ is the average refractive index, for barium ferrite, $\bar{n} \approx 2.8$ [19] in the visible range, λ is the wavelength of the light wave in vacuum.

By inserting the quantum-mechanical expressions for the electric susceptibility into equation (3), we obtain

$$\theta_{\mathrm{F}} = \frac{N\pi(\bar{n}^2+2)^2 e^2}{9c\bar{n}\hbar} \frac{8\pi}{3} \left(\langle r \rangle_{3d4p}\right)^2 \times \sum_{ng} B_{ng} \frac{\omega^2(\omega_{ng}^2 - \omega^2 - \Gamma_{ng}^2)}{(\omega_{ng}^2 - \omega^2 - \Gamma_{ng}^2)^2 + 4\omega^2\Gamma_{ng}^2} \rho_g \tag{4}$$

for each type of non-equivalent ion present in the material, where

$$\frac{8\pi}{3} \left(\langle r \rangle_{3d4p}\right)^2 B_{ng} = |\langle n| V_- |g\rangle|^2 - |\langle n| V_+ |g\rangle|^2 . \tag{5}$$

In equations (4, 5), N is the number of the magnetic ions per crystal site per unit volume, c the velocity of the light in vacuum, ω the angular frequency of the light wave, Γ_{ng} is the half-width of resonance lines. g runs over ground states with occupation probability ρ_g and n runs over states at energies $\hbar\omega_{ng}$ above the ground states. $eV_\pm$ are the electric dipole moment operators for right- and left-hand circularly polarized light, respectively, and are written:

$$eV_\pm = \sum_i e(x_i \pm j y_i). \tag{6}$$

When the angular frequency ω is far from the resonance frequencies, *i.e.* when $|\omega_{ng}^2 - \omega^2| \gg \Gamma_{ng}^2$, the frequency factor in equation (4) can be reduced to $\omega^2/(\omega_{ng}^2 - \omega^2)$.

To calculate the contribution of the intra-ionic electric dipole transitions between the ground and the parity allowed excited configurations to the Faraday rotation, it is necessary to calculate the splitting of these configurations under the crystal field and superexchange interaction. In the case of the Ni^{2+} ion, the ground and lowest parity allowed excited configurations are $3d^8$ and $3d^7 4p$ configurations, respectively. So, $|g\rangle$ ($|n\rangle$) states in equation (5) are the split $3d^8$ ($3d^7 4p$) states.

The Hamiltonian of a Ni^{2+} ion in the crystal is

$$H = H_0 + H_{\mathrm{SO}} + H_{\mathrm{C}} + H_{\mathrm{ex}}, \tag{7}$$

where H_{SO} is the spin-orbit (SO) interaction, $H_0 + H_{\mathrm{SO}}$ is the Hamiltonian of a free Ni^{2+} ion, H_{C} and H_{ex} are the crystal field (CF) and superexchange interaction Hamiltonians, respectively. In this paper, only the spontaneous Faraday rotation will be studied, so the external magnetic field has not to be considered. The crystal field Hamiltonian can be expressed as

$$H_{\mathrm{C}} = \sum_{kq} \sum_{i} A_{kq} r^k Y_{kq}(\theta_i, \varphi_i), \tag{8}$$

where $A_{kq} r^k$ are the crystal field parameters, $Y_{kq}(\theta, \varphi)$ are spherical harmonics. According to reference [9], the Ni^{2+} ions in the Ni-substituted barium ferrite replace the Fe^{3+} ions, so they may occupy the five crystal sites ($2a$, $2b$, $4f_1$, $4f_2$, and $12k$). In the calculations, the values of $\langle r \rangle_{3d4p}$, $\langle r^2 \rangle_{3d}$, $\langle r^3 \rangle_{3d}$, $\langle r^4 \rangle_{3d}$, $\langle r^2 \rangle_{4p}$ of the Ni^{2+} ions and the crystal field parameters were calculated by the Slater radial wave function of the free Ni^{2+} ion and the point charge model. The non-zero parameters of the even-parity crystal field acting on the $3d$ electrons of the $2b$ site Fe^{3+} ions are $A_{20}\langle r^2 \rangle_{3d} = -14\,966\ \mathrm{cm}^{-1}$, $A_{40}\langle r^4 \rangle_{3d} = 13\,197\ \mathrm{cm}^{-1}$, the corresponding non-zero parameter for the $4p$ electrons is $A_{20}\langle r^2 \rangle_{4p} = -66\,386\ \mathrm{cm}^{-1}$. Here the z axis is taken to be along the c axis of the hexagonal structure of the barium ferrite crystal. The numbers of the non-zero parameters of the even-parity crystal field upon the Fe^{3+} ions at other sites are larger. We would like to point out that in some of our previous papers [20,21], the magnetocrystalline anisotropy of the barium ferrite and Zn_2W ferrite has been well-explained theoretically by using the same method. So, it is a reasonable choice.

In this paper, the mean field approximation is used. So, the superexchange interaction H_{ex} is expressed as

$$H_{\mathrm{ex}} = 2\mu_{\mathrm{B}} H_{\mathrm{exch}} \sum_i s_{zi} = 2\mu_{\mathrm{B}} H_{\mathrm{exch}} S_z, \tag{9}$$

where S_z is the z-component of the total spin angular moment operator, and H_{exch} is the exchange field. It should be noted that the exchange field is not identical to the classical molecular field H_{m}. When only the lowest multiplet is to be considered, the superexchange interaction is usually expressed as

$$H_{\mathrm{ex}} = \mu_{\mathrm{B}} g_J H_{\mathrm{m}} J_z, \tag{10}$$

where J_z is the z-component of the total angular moment operator and g_J is the Lande factor. It is seen that $H_{\mathrm{exch}}/H_{\mathrm{m}} = \langle L_z + 2S_z \rangle / \langle 2S_z \rangle$, here $\langle S_z \rangle$ indicates the expectation value of the operator S_z in a state. Guillot *et al.* [22] have deduced from the magnetic measurements that the molecular field acting on the Fe^{3+} ions in yttrium iron garnet is about 4000 kOe. For the Fe^{3+} ions, the orbit angular moment of the ground term (^5S term) is zero. Consequently, for the ground term of the Fe^{3+} ions, the exchange field is equal to the molecular field. Furthermore, the Neel temperature of the barium ferrite is higher than that of the yttrium iron garnet and the characteristics of the Ni^{2+} and Fe^{3+} ions are very close. So the magnitude of the exchange field acting on the Ni^{2+} ions in the barium ferrite is estimated to be 5000 kOe. The above value is for the exchange field upon the $3d$ electrons. When we calculate the diamagnetic Faraday rotation (Sect. 2.2) in the Ni-substituted barium ferrite, it is necessary to determine the strength of the superexchange interaction on the excited configuration. To our knowledge, there is no theoretical or experimental information about the magnitude of the interaction involving the $4p$ electrons. The average space expansion of the $4p$ wave function is larger than that of the $3d$ wave function, and the superexchange interaction of the Fe^{3+} ions with the $4p$ electrons of the Ni^{2+} ions is larger than that with the $3d$ electrons of the Ni^{2+} ions. So, in our calculation, the exchange field on the $4p$ electrons has been estimated to be four times stronger than that on the $3d$ electrons. Since $3d^7 4p$ configuration has seven $3d$ electrons and only one $4p$ electron, the influence of the correctness of this estimation on the calculated results is small.

2.1 "Paramagnetic type" Faraday rotation

The ground configuration of a free Ni^{2+} ion has a ^3F term as the ground term with another spin triplet term ^3P and other higher-lying spin singlet terms. According to the book by Moore [23], the energies of the three multiplets $^3F_4$, $^3F_3$, $^3F_2$ of the ^3F term are 0, 1361, 2270 cm^{-1}, respectively; those of $^3P_2$, $^3P_1$, $^3P_0$ multiplets are 16 662, 16 978, 17 231 cm^{-1}, respectively. Note that all these values were determined by optical spectroscopy. The even-parity-CF and spin-orbit interaction split energy levels and the corresponding wave functions of these two triplet terms were obtained by solving the following secular equation,

$$|| \langle L, J, J_z | H_0 + H_{\mathrm{SO}} + H_{\mathrm{C}} | L', J', J_z' \rangle - E\delta_{LL'}\delta_{JJ'}\delta_{J_z J_z'} || = 0, \tag{11}$$

the bra and ket included all the states of these two terms. For the Ni^{2+} ion at the $2b$ site, these two terms are split into 18 levels, among which six levels are singlets, others are double degenerate. The energies of the lowest twelve levels, whose main components are ^3F states, are shown in Table 1. It should be noted that in this paper the energy of the $^3F_4$ multiplet of the ground configuration is always

Table 1. The energies (in cm^{-1}) of the lowest twelve even-parity-CF and SO split levels of the ground configuration of the Ni^{2+} ion at the 2*b* site. In this and all other tables the energy of the multiplet $^3F_4$ of the ground configuration of a free Ni^{2+} ion is taken to be zero.

−3456	−2903	−2195	246.8	1341	1561*
1711	2010	2281	2591*	3145	3521*

*The three levels with a star are singlets, others are double degenerate.

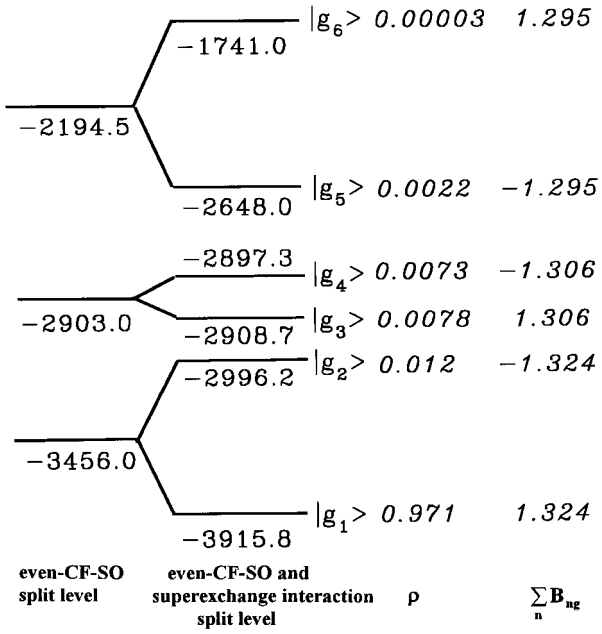

Fig. 1. Energy schema of the lowest 6 even-parity-CF-SO and superexchange-interaction split $3d^8$ levels of the Ni^{2+} ions at the 2*b* site; the values of the energy (in cm^{-1}), room temperature occupation probability ρ, and $\sum_n B_{ng}$ (its meaning will be given in Sect. 4) related with the considered levels being given. In this and all other figures the energy of the multiplet $^3F_4$ of the ground configuration of a free Ni^{2+} ion is taken to be zero.

taken to be zero. The lowest three levels are double degenerate. From Table 1 it can be seen that the energy gaps between these three levels and other levels are large. Furthermore, because of the selection rules the lowest level (−3 456 cm^{-1}) can be mixed only with the fifth level (1341 cm^{-1}) while the second (third) level can be mixed only with the eighth and ninth (seventh and eleventh) levels by the exchange field. Therefore only the first order Zeeman effect of the lowest three levels is important. The energies and the occupation probabilities at 300 K of the lowest six even-parity-CF-SO and superexchange-interaction split levels are given in Figure 1. It should be noted that the room temperature occupation probability of the third CF-SO and superexchange-interaction split level is already less than 1 percent.

However, for the Ni^{2+} ions at other crystal sites, the situation is not so simple because the high order perturbation correction of the superexchange interaction can not be neglected. As a result, the CF-SO and superexchange-interaction split levels and the corresponding wave functions have then to be obtained by solving the following secular equation:

$$|| \langle \varphi_i | H_0 + H_{\rm SO} + H_{\rm C} + H_{\rm ex} | \varphi_j \rangle - E\delta_{ij} || = 0. \quad (12)$$

Here the bra and ket include the states of some low-lying CF and SO split levels; the diagonal matrix elements $\langle \varphi_i | H_0 + H_{\rm SO} + H_{\rm C} | \varphi_i \rangle$ are the energies of these levels.

The $3d^7 4p$ configuration has many terms. Among them the terms allowed by the electric dipole transitions from $3d^8$: ^3F term are: $3d^7(^4F)4p$: ^3G, ^3F, ^3D; $3d^7(^4P)4p$: ^3D; $3d^7(^2P)4p$: ^3D; $3d^7(^2D1)4p$: ^3F, ^3D; $3d^7(^2D2)4p$: ^3F, ^3D; $3d^7(^2F)4p$: ^3G, ^3F, ^3D; $3d^7(^2G)4p$: ^3G, ^3F; $3d^7(^2H)4p$: ^3G. According to reference [23], the lowest three terms are $3d^7(^4F)4p$: ^3G, ^3F and ^3D. The average energies of these three terms are 116 328, 117 003 and 119 359 cm^{-1}, respectively. The energy gaps between these three terms are less than 3 000 cm^{-1}. So, in calculating the crystal field splitting of these terms, the mixing of them has to be considered. The energies of other higher-lying terms are found to be about 20 000 cm^{-1} higher than those of these three terms, but the assignment of the levels remains doubtful. Therefore, the energies of all these higher-lying terms are supposed to be 130 000 cm^{-1} and the CF splitting of them is neglected. Since the energy gaps between these terms are small compared with the energy difference between them and the $3d^8$: ^3F term, the error due to the above approximation is small.

The even-parity-CF and SO split energy levels and the corresponding wave functions of the $3d^7(^4F)4p$: ^3G, ^3F, ^3D terms were also obtained by solving equation (11). The bra and ket included all states of these three terms. The values of the diagonal matrix elements $\langle L, J, J_z | H_0 + H_{\rm SO} | L, J, J_z \rangle$ were taken from reference [23]. For the Ni^{2+} ions at the 2*b* site, these three terms are split into 36 levels; most of them are double degenerate, others are singlets. Their energies are found in the 96 229 ∼ 130 580 cm^{-1} range. In this subsection, the Zeeman effect of the $3d^7 4p$ configuration induced by the superexchange interaction is neglected and the paramagnetic Faraday rotation will be obtained [16].

The calculated room temperature paramagnetic Faraday rotation contributed by the Ni^{2+} ions assuming that all the Ni^{2+} ions are at the 2*b* sites is shown in Table 2, for various photon energies. The 496 nm wavelength paramagnetic Faraday rotation is 15 256 degr cm^{-1}/x. The meaning of x has been given at the beginning of Section 1. The calculated curve of $(\bar{n}^2+2)^2\pi\varepsilon''_{xy}/(9\lambda\bar{n})$ *versus* photon energy produced by the Ni^{2+} ions at the 2*b* sites is shown in Figure 2. It should be noted that these results include the contributions of all the spin triplet terms of the $3d^7 4p$ configuration. Since, in our calculation, $\bar{n}$ is supposed to be a constant, it is easy to change this curve into a ε''_{xy} spectrum. At low energy range, where the absorption is

Table 2. The paramagnetic, diamagnetic and full Faraday rotation (FR) produced by the Ni^{2+} in $Ba_{1-x}M_xFe_{12-x}Ni_xO_{19}$ at 300 K (in degr cm^{-1}/x) assuming that all the Ni^{2+} ions are distributed over the 2*b* sites. The full Faraday rotation calculated without taking the mixing of different multiplets of the ground term into account is noted as "full FR*".

photon energy (eV)	1	2	2.5	4	6
para FR	2399	9692	15 256	40 351	97 220
dia FR	34	141	224	623	1677
full FR	2436	9842	15 496	41 016	99 014
full FR*	1083	4369	6871	18 100	43 112

small, this curve is identical to the paramagnetic Faraday rotation spectrum.

Now we will try to get more insight into the processes responsible for this strong MO enhancement, taking the Ni^{2+} ions at the 2*b* sites as an example. It can be seen from the occupation probabilities of various levels reported in Figure 1 that, at and below room temperature, the Faraday rotation almost fully comes from the transitions from the lowest two even-parity-CF-SO and superexchange-interaction split $3d^8$ states $|g_1\rangle$ and $|g_2\rangle$ to the $3d^7 4p$ levels. Among the 36 CF-SO split $3d^7(^4F)4p$: ^3G, ^3F, ^3D levels, there are 11 double degenerate levels, to which the electric dipole transitions from $|g_1\rangle$ and $|g_2\rangle$ are permitted by the selection rule. However, only three levels of them whose energies are 99 027, 99 030, and 120 793 cm^{-1}, respectively, yield large contributions to the Faraday rotation. The two orthogonal states of the level located at 99 027 cm^{-1} are expressed as $|n_1\rangle$ and $|n_2\rangle$, the orthogonal states of other two levels are expressed as $|n_3\rangle \ldots |n_6\rangle$ (see Fig. 3a). It can be deduced that the transitional matrix element $B_{n_1g_1}$ associated with the transition from $|g_1\rangle$ state to $|n_1\rangle$ state has the same magnitude and is of opposite sign with the transitional matrix element $B_{n_2g_2}$ associated with the transition from $|g_2\rangle$ to $|n_2\rangle$. It can be deduced easily from the wave functions that $B_{n_2g_1}$ and $B_{n_1g_2}$ equal zero. Hence, if the degeneracy of the $|g_1\rangle$ and $|g_2\rangle$ states is not lifted by the superexchange interaction, the electric dipole transitions between $|g_1\rangle$ and $|g_2\rangle$ states and the two orthogonal states $|n_1\rangle$ and $|n_2\rangle$ will have no net contribution to the MO effect. The above conclusions about the transitional matrix elements can be extended to other CF and SO split double degenerate $3d^7 4p$ levels. Finally, we arrive at the conclusion that if there is no Zeeman effect in both the ground and excited configurations, there will be no MO effect.

But the Zeeman splitting makes the occupation probabilities of the sublevels of one CF and SO split $3d^8$ level different (see Fig. 3b). Now we define $\theta_F(ng)$ as the Faraday rotation induced by the electric dipole transition from

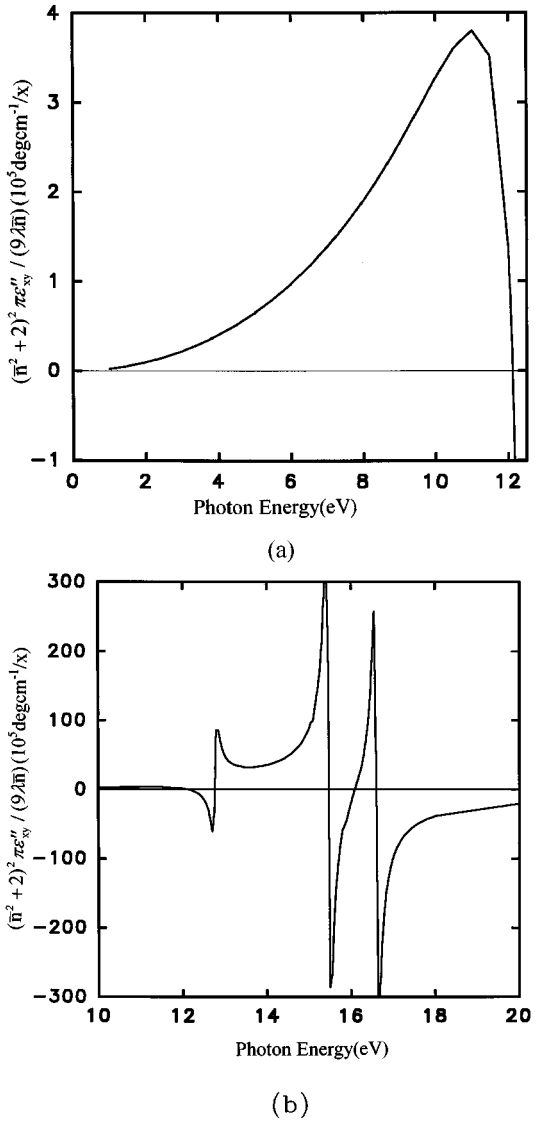

Fig. 2. The calculated room temperature paramagnetic $(\bar{n}^2+2)^2\pi\varepsilon''_{xy}/(9\lambda\bar{n})$ spectrum produced by the Ni^{2+} ions in $Ba_{1-x}M_xFe_{12-x}Ni_xO_{19}$ when all of them are distributed over the 2*b* sites; (a) below 12 eV photon energy, (b) above 12 eV photon energy.

any ground configuration state $|g\rangle$ to one excited configuration state $|n\rangle$. Obviously, $\theta_F(ng)$ is given by one term on the right side of equation (4). We would like to recall that equations (3, 4) stand only when the optical absorption is weak. Therefore, at high photon energy, $\theta_F(ng)$ should be read as $\frac{1}{9}(\bar{n}^2+2)^2\frac{\pi}{\lambda\bar{n}}\varepsilon''_{xy}$. Because of the effect of the superexchange interaction on the ground configuration, the resonance frequencies of the transition from $|g_1\rangle$ to $|n_1\rangle$ ($\omega_{n_1g_1}$) and the transition from $|g_2\rangle$ to $|n_2\rangle$ ($\omega_{n_2g_2}$) are now different. But the difference is very small. In a good approximation, all the factors in the expressions of the absolute values of the Faraday rotations, $|\theta_F(n_1g_1)|$ and $|\theta_F(n_2g_2)|$, induced by these two transitions will be the same except the occupation probability factor (see Eq. (4)). Hence, at a given wavelength, the difference

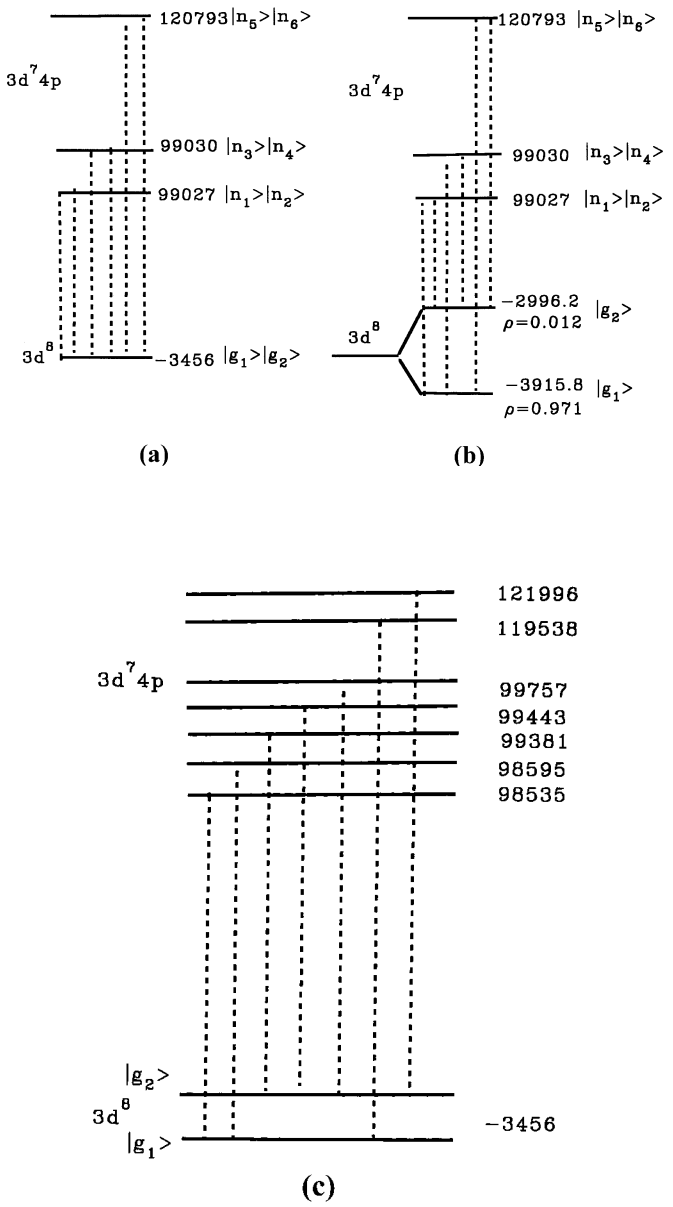

Fig. 3. The split $3d^8$ and $3d^7 4p$ levels, which are important in the producing of the MO effect, and the electric dipole transitions between them. The data on the right side are the energy values (in cm^{-1}). $|g_1\rangle$, $|g_2\rangle$, $|n_1\rangle$, $\ldots|n_6\rangle$ express the orthogonal states of considered levels. (a) The even-parity-CF-SO-split $3d^8$ and $3d^7 4p$ levels. No MO effect exists because there is no Zeeman splitting. (b) The even-parity-CF-SO split $3d^7 4p$ levels and the even-parity-CF-SO and superexchange-interaction-split $3d^8$ levels, the transitions between them result in the paramagnetic MO effect. ρ indicates the occupation probabilities of the considered levels. (c) The lowest even-parity-CF-SO-split $3d^8$ level and the even-parity-CF-SO and superexchange-interaction-split $3d^7 4p$ levels, the transitions between them give rise to the diamagnetic MO effect. Please note that $|g_1\rangle$ and $|g_2\rangle$ states have the same energy.

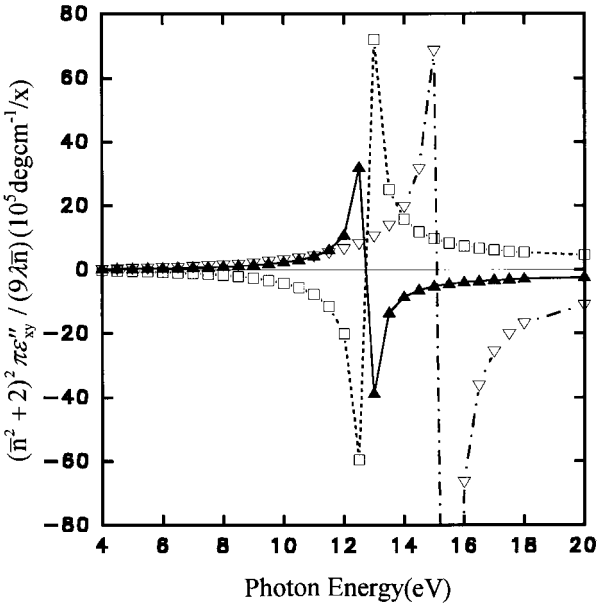

Fig. 4. The calculated room temperature paramagnetic $(\bar{n}^2+2)^2\pi\varepsilon''_{xy}/(9\lambda\bar{n})$ spectra contributed by the Ni^{2+} ions in $Ba_{1-x}M_xFe_{12-x}Ni_xO_{19}$ assuming that all of them are distributed over the $2b$ sites; $(-\blacktriangle-)$ caused by the $3d^7 4p$ level with energy 99 027 $\mathrm{cm}^{-1} \rightarrow 3d^8$ states transitions; $(\cdots\square\cdots)$ caused by the $3d^7 4p$ level with energy 99 030 $\mathrm{cm}^{-1} \rightarrow 3d^8$ states transitions; $(-\nabla-)$ caused by the $3d^7 4p$ level with energy 120 793 $\mathrm{cm}^{-1} \rightarrow 3d^8$ states transitions.

between the two occupation probabilities, ρ_{g_1} and ρ_{g_2}, leads to the MO effect, and the variation of the difference of $|\theta_F(n_1 g_1)|$ and $|\theta_F(n_2 g_2)|$ *versus* wavelength gives the $\frac{1}{9}(\bar{n}^2+2)^2\frac{\pi}{\lambda\bar{n}}\varepsilon''_{xy}$ spectrum. For the Ni^{2+} ions at the $2b$ site, the difference between the occupation probabilities of the two sublevels of the lowest CF and SO split $3d^8$ level is so large (at room temperature it is 0.959) that the Faraday rotation induced by the $3d^n \rightarrow d^{n-1}4p$ transitions is very large even far from the resonance frequencies when the frequency factor in equation (4) becomes small.

Such a Faraday rotation is usually called a paramagnetic type of Faraday rotation. It's magnitude usually depends sensitively on temperature through the occupation probability factor. The spectra of $\frac{1}{9}(\bar{n}^2+2)^2\frac{\pi}{\lambda\bar{n}}\varepsilon''_{xy}$ (see Eq. (3)) caused by the electric dipole transitions from the lowest two CF-SO and superexchange-interaction split $3d^8$ levels to the three CF-SO split $3d^7 4p$ levels mentioned above are shown in Figure 4.

2.2 "Diamagnetic type" Faraday rotation

The origin of the so-called diamagnetic type of Faraday rotation can be interpreted schematically as follows. Suppose: (1) the Zeeman effect of the ground configuration is neglected; (2) in the excited configuration, either two nondegenerate CF-SO split states or two states of a double degenerate CF-SO split level are present. These two states will be mixed with each other or split by the superexchange interaction. We use $|n_1\rangle$ and $|n_2\rangle$ to express these

two CF-SO split and superexchange-interaction mixed (or split) states, and suppose that the lowest CF-SO split level of the ground configuration is double degenerate and its two orthogonal states are $|g_1\rangle$ and $|g_2\rangle$. Now if the sum $B_{n_1g_1} + B_{n_1g_2}$ is different from zero, then the two quantities $B_{n_1g_1} + B_{n_1g_2}$ and $B_{n_2g_1} + B_{n_2g_2}$ will always have the same magnitude and opposite signs. Because the two states $|g_1\rangle$ and $|g_2\rangle$ have the same energy value, the resonance frequencies $\omega_{n_1g_1}$ and $\omega_{n_1g_2}$ related to the two transitions $|g_1\rangle \rightarrow |n_1\rangle$ and $|g_2\rangle \rightarrow |n_1\rangle$ are the same and can be noted as ω_{n_1g}. For the same reason, the resonance frequencies corresponding to the transitions $|g_1\rangle \rightarrow |n_2\rangle$ and $|g_2\rangle \rightarrow |n_2\rangle$ are the same and are noted as ω_{n_2g}. Whereas, because of the Zeeman effect of the excited configuration, the energy of the two states $|n_1\rangle$ and $|n_2\rangle$ and then the two resonance frequencies ω_{n_1g} and ω_{n_2g} are slightly different. Consequently, the absolute values of $[\theta_F(n_1g_1) + \theta_F(n_1g_2)]\rho_g$ and $[\theta_F(n_2g_1) + \theta_F(n_2g_2)]\rho_g$ (ρ_g is the occupation probability of $|g_1\rangle$ and $|g_2\rangle$) have the same functional relation with the frequency ω except the small difference between ω_{n_1g} and ω_{n_2g}; and the variation of the sum of these two quantities *versus* the frequency presents a narrow peak. Sometimes the involved CF-SO split ground configuration level is nondegenerate, then $|g_1\rangle$ and $|g_2\rangle$ mentioned above will indicate the same state and the same conclusion can be derived.

In the following, we analyse the diamagnetic MO effect caused by the Ni^{2+} ions at the 2*b* sites. We recall that (Sect. 2.1), for the ground configuration, only the two states $|g_1\rangle$ and $|g_2\rangle$ (see Figs. 1 and 3c) are important in producing the Faraday rotation; for the $3d^7(^4F)4p$: ^3G, ^3F, ^3D terms, only eleven double degenerate CF-SO split levels have contributions to the Faraday rotation. It can be shown that the mixing of these 11 double degenerate CF-SO split $3d^74p$ levels induced by the superexchange interaction is not negligible, though they can not be mixed with other CF-SO split $3d^74p$ levels. Hence in the calculation of the Zeeman splitting, the higher order perturbation correction has to be taken into account. These 11 levels are split into 22 nondegenerate levels. Among them, the 7 levels, whose energies are reported in Figure 3c, have a large contribution to the MO effect. The electric dipole transitions from the two orthogonal states $|g_1\rangle$ and $|g_2\rangle$ of the lowest double degenerate CF-SO split $3d^8$ level to these 7 levels are shown in Figure 3c as well. From Figure 3c, it can be found that these 7 levels can be divided into two groups, the five levels located just below 100 000 cm^{-1} compose a group, the other two levels (119 538 and 121 996 cm^{-1}) compose another one. A detailed calculation has shown that the transitions from $|g_1\rangle$ and $|g_2\rangle$ states to the five states of the first group produce a narrow positive peak around 12.7 eV photon energy in the $\frac{1}{9}(\bar{n}^2+2)^2\frac{\pi}{\lambda\bar{n}}\varepsilon''_{xy}$ spectrum. Similarly, the transitions from $|g_1\rangle$ and $|g_2\rangle$ states to the two states in the second group result in a narrow negative peak around 15.4 eV.

Other higher-lying terms of the $3d^74p$ configuration also have contributions to the MO effect. The wave functions and energies of the superexchange-interaction split levels of these terms were also obtained by solving equation (12). However, in the calculation, all the multiplets of these terms were supposed to have the same energy value (130 000 cm^{-1}) and the crystal field effect was neglected. These superexchange-interaction split levels lead to a positive peak around 16.5 eV (133 456 cm^{-1}) photon energy. The so determined room temperature diamagnetic $\frac{1}{9}(\bar{n}^2+2)^2\frac{\pi}{\lambda\bar{n}}\varepsilon''_{xy}$ spectrum is shown in Figure 5. As mentioned above, the peak around 16.5 eV is associated with the higher lying $3d^74p$ terms. The neglection of the energy differences between the different multiplets of these terms means that the spin-orbit interaction in these terms is taken to be zero. Therefore in this figure, the spectrum above 16.2 eV is shown by a dotted curve. The other peaks are associated with the $3d^7(^4F)4p$: ^3G, ^3F, ^3D terms. For these terms, the energies of various multiplets were taken from reference [23]. This means that the spin-orbit interaction in these terms was taken to be the value determined by optical spectroscopy [23]. So in Figure 5, the spectrum below 16.2 eV is shown by a solid curve. The meaning of the dotted curve below 16.2 eV will be given in the last part of Section 4.

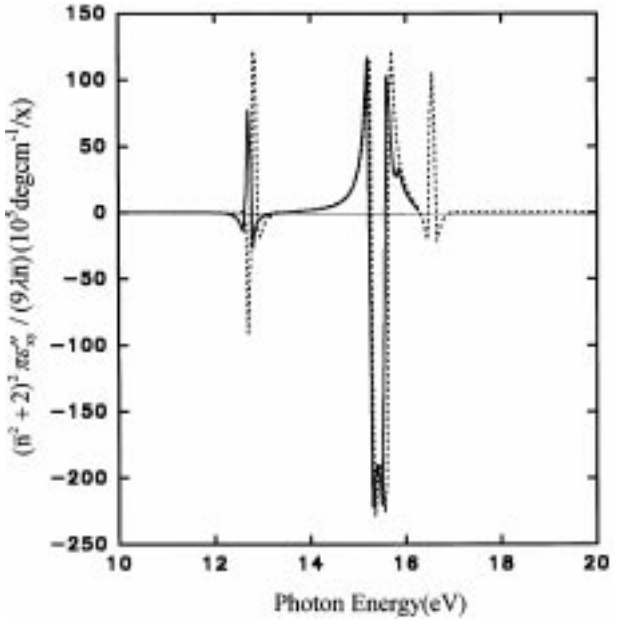

Fig. 5. The calculated room temperature diamagnetic $(\bar{n}^2+2)^2\pi\varepsilon''_{xy}/(9\lambda\bar{n})$ spectra contributed by the Ni^{2+} ions in $Ba_{1-x}M_xFe_{12-x}Ni_xO_{19}$ assuming that all of them are distributed over the 2*b* sites. Solid curve is the spectrum obtained assuming that the spin-orbit interaction in the excited configuration is taken to be the actual value. Dotted curve is the spectrum obtained supposing that the corresponding interaction is absent. In both cases the spin-orbit interaction in the ground configuration is taken to be the actual value.

The calculated diamagnetic Faraday rotations below 6 eV photon energy at 300 K are listed in Table 2. Since the peaks of diamagnetic Faraday rotation are very narrow, the diamagnetic Faraday rotation is important only in the vicinity of the peaks, it being very small in the visible range. Finally, we would like to recall that in our calculation the exchange field on the 4*p* electrons has been

Table 3. The calculated full Faraday rotation $\theta_{\rm F}$ (in $\mathrm{degr\,cm^{-1}}/x$) at 496 nm (2.5 eV photon energy) and 300 K contributed by the Ni^{2+} ions in $Ba_{1-x}M_xFe_{12-x}Ni_xO_{19}$ when all of them are distributed over one equivalent crystal site (for example, when all the Ni^{2+} ions are at the $2a$ sites, $\theta_F = 1970\ \mathrm{degr\,cm^{-1}}/x$).

site	$2a$	$2b$	$4f_1$	$4f_2$	$12k$
$\theta_{\rm F}$	1970	15 496	−14 500	−4610	3890

estimated to be four times stronger than that on the $3d$ electrons. Such an estimation is somewhat arbitrary. However, the obtained main features are not sensible to this value.

2.3 Full Faraday rotation and the influence of the mixing of different ground term multiplets

As discussed in the preceding two subsections, the paramagnetic MO effect is produced by the occupation probability difference caused by the Zeeman effect of the ground configuration, while the diamagnetic MO effect is produced by the resonance frequency difference induced by the Zeeman effect of the excited configuration. When the Zeeman effect of both the ground and excited configurations is taken into account, the full Faraday rotation is obtained. The full Faraday rotation (at 300 K) below 6 eV photon energy contributed by the Ni^{2+} ions in $Ba_{1-x}M_xFe_{12-x}Ni_xO_{19}$, assuming all of them are distributed over the $2b$ sites, are reported in Table 2. It can be seen that, when far from the MO resonance frequencies, the full Faraday rotation is almost fully determined by the paramagnetic components.

The full Faraday rotations at 496 nm and 300 K produced by the Ni^{2+} ions distributed over other equivalent crystal sites in $Ba_{1-x}M_xFe_{12-x}Ni_xO_{19}$ (for example, all the Ni^{2+} ions are at the $4f_1$ sites) are also almost determined by the paramagnetic components and their calculated values are shown in Table 3. The MO enhancement factors of the Ni^{2+} ions at $2b$ and $4f_1$ sites are near the observed values [9]. According to Machida *et al.* [3] and Gomi *et al.* [9], the Faraday rotation induced by a Fe^{3+} ion in the barium ferrite is much smaller than that by a Ni^{2+} ion at the $2b$ or $4f_1$ site. Therefore, in explaining the enhancement by Ni^{2+} substitution, it has been neglected to a first-order approximation. It should be noted that, in our calculation, the values of $\langle r\rangle_{3d4p}$, $\langle r^2\rangle_{3d}$ etc. are obtained with the Slater radial wave function of the free Ni^{2+} ions. It is expected that the extension of the radial wave function of the Ni^{2+} ion in the crystal will make the actual enhancement factor larger than that given above. It is worthwhile to pointing that, as mentioned above, the Slater radial wave function and the point-charge model were used to calculate the magneto-crystalline anisotropy of the barium ferrite [20] and Zn_2W ferrite [21]. Although the calculated results can explain the main observed results well, the magnitudes of the calculated magneto-crystalline anisotropy constant K_1 are smaller than the observed ones. This fact also makes us believe that the actual enhancement factors will be larger than the values given above. Finally, we can conclude that the intra-ionic electric dipole transition is an important origin of the large MO enhancement of the Ni^{2+} substitution in the barium ferrite.

In many theoretical works on MO effects (see [18]), for the ground configuration, only the lowest multiplet is considered. However, when higher-lying ground term multiplets are taken into account, the energy schema and the wave functions of the split levels will be modified. Then the difference of the occupation probabilities of the low-lying split ground configuration levels and the values of B_{ng} associated with these levels are changed. Consequently, the mixing of different ground term multiplets induced by the crystal field has a great influence on the Faraday rotation and has been taken into account in our calculations. The Ni^{2+} ion (at the $2b$ site) contribution to the full Faraday rotation (at 300 K) below 6 eV photon energy calculated without taking such a mixing into account is listed in Table 2. The data show that such an influence is very important.

3 Intra-ionic 3d → 3d electric dipole transition induced by odd parity crystal field

Because the environment of the $2b$ site in barium ferrite has no center of symmetry, we take the Ni^{2+} ions at the $2b$ site as an example to study the contribution of the intra-ionic $d \to d$ electric dipole transitions induced by the odd parity crystal field to the Faraday rotation. The non-zero parameters of the odd parity crystal field acting on the Ni^{2+} ions at the $2b$ site are $A_{3\pm3}\langle r^3\rangle = \mp 38\,363.7\ \mathrm{cm^{-1}}$, which are also determined by the point charge model and the Slater radial wave function. The matrix elements of the odd parity CF induced transitions between the $3d^8$ ground states (expressed as $|3d^8_g\rangle$) and $3d^8$ excited states (expressed as $|3d^8_{\rm ex}\rangle$) can be expressed as

$$\frac{1}{E_{3d^7 4p} - E_{3d^8_{\rm ex}}} \langle 3d^8_{\rm ex}\,|H_{\rm C_{odd}}|\,3d^7 4p\rangle\langle 3d^7 4p\,|V_{\pm}|\,3d^8_g\rangle, \tag{13}$$

where $E_{3d^7 4p}$ is the energy of an even-parity-CF-SO split $|3d^7 4p\rangle$ state, $E_{3d^8_{\rm ex}}$ and $E_{3d^8_g}$ are the energy of the high-lying and low-lying even-parity-CF-SO and superexchange-interaction split $3d^8$ states ($|3d^8_{\rm ex}\rangle$, $|3d^8_g\rangle$), respectively.

There are many such high-order processes for the Ni^{2+} ions and the calculation is very tedious. As mentioned in Section 2.1, in the $3d^7 4p$ configuration, the lowest three spin triplet terms ($3d^7(^4F)4p$: ^3G, ^3F, ^3D) are about 20 000 $\mathrm{cm^{-1}}$ lower than other spin triplet terms. So for simplicity's sake, in the study of the contribution of the intra-ionic $3d \to 3d$ electric dipole transitions to the Faraday rotation, only these three terms of the $3d^7 4p$ configuration are considered. We obtained the even- and odd-parity-CF and SO split levels of the $3d^8$ and $3d^7 4p$

configurations by solving equation (11). Now the crystal field Hamiltonian H_C included both the even and odd-parity terms, the bra and ket included all the states of the spin triplet terms (^3F, ^3P) of the $3d^8$ configuration and the $3d^7(^4F)4p$: ^3G, ^3F, ^3D terms of the $3d^74p$ configuration.

There are eight nondegenerate and eleven double degenerate odd- and even-CF and SO split levels whose main components are $3d^8$ states. Their energies were found in the range from -4721 to 17 752 cm^{-1}. Similar to the situation without taking the odd-parity crystal field terms into account, for the low-lying states, only the lowest double degenerate CF-SO split level (-4721 cm^{-1}) yields a great contribution to the Faraday rotation. This level is split into two sublevels (located at -5178 and -4264 cm^{-1}) by the superexchange interaction. There are two higher-lying double degenerate even- and odd-parity-CF and SO split levels whose main components are $3d^8$ states and their energies are 13 739 and 17 513 cm^{-1} respectively , the electric dipole transitions between them and the lowest two $3d^8$ levels mentioned above have non-negligible contribution to the Faraday rotation. It can be shown that: (1) the two levels, whose energies are 13 739 and 17 513 cm^{-1} respectively, contain non-negligible components of $4p$ wave functions, the involved transitions actually are $3d \rightarrow 4p$ transitions. (2) The main components of the lowest two levels (at -5178 and -4264 cm^{-1}) are $3d^8$ ^3F states, while those of the two higher-lying levels mentioned above are $3d^8$ ^3P states. So the transitions between them are usually called $(3d)^3F \rightarrow (3d)^3P$ or simply $d \rightarrow d$ transitions. (3) The mixing of the $3d^8$ and $3d^74p$ configurations induced by the odd-parity crystal field terms is not strong. Hence such $d \rightarrow d$ transitions are very weak. The Faraday rotation spectra caused by the electric dipole transitions mentioned above are shown in Figure 6. From this figure, it can be seen that the odd-parity crystal field upon the Ni^{2+} ions at the $2b$ site does produce MO resonance around 2.5 eV photon energy. However, the maximum values of the Faraday rotation near the resonance frequencies are less than 1000 degr cm^{-1}/x, assuming that all the Ni^{2+} ions are distributed over the $2b$ sites. It is too small to explain the observed Faraday rotation at this wavelength range.

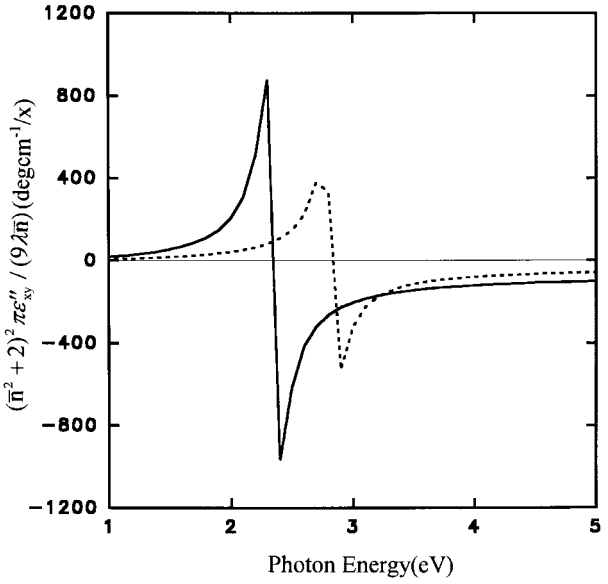

Fig. 6. Calculated room temperature Faraday rotation spectra produced by the electric dipole transitions from the lowest two even- and odd-parity-CF-SO- and superexchange-interaction split levels to the even- and odd-parity-CF and SO split levels, whose energies are 13 739 cm^{-1} (solid curve) and 17 513 cm^{-1} (dotted curve), respectively, of the Ni^{2+} ions in $Ba_{1-x}M_xFe_{12-x}Ni_xO_{19}$ assuming that all of them are distributed over the $2b$ sites.

4 Role of spin-orbit interaction in MO effects

Early in 1932, Hulme [24] deduced that for a ferromagnetic material the spin-orbit interaction of the excited states was needed to produce non-zero MO effects. To our knowledge, the first quantitative analysis about the role of the spin-orbit coupling in the MO effects was made by Misemer [25] for MnBi. From the theoretical calculations, he arrived at the conclusion that when all other parameters were held fixed, the MO coefficient grew approximately linearly with increasing strength of the spin-orbit interaction. Later, Oppeneer *et al.* [26] showed that in transition metals Fe, Co, and Ni, the MO Kerr effect scaled linearly with the spin-orbit coupling but was a rather complex function of magnetization. Recently, Dionne *et al.* [27] made a molecular-orbital analysis for the MO enhancement of Bi in Bi-substituted yttrium iron garnets; the giant MO enhancement was attributed to the large splitting of the excited states induced by the spin-orbit interactions. However, detailed quantitative studies about the effect of the spin-orbit interaction on the MO effects in such complex systems like the garnets do not exist. In this section, we will analyse this problem using quantum theory, choosing the Ni^{2+} ions at the $2b$ site of barium ferrite as an example.

We define two relative spin-orbit interaction constants: ξ_1 is the ratio of the assumed strength to the actual strength of the spin-orbit interaction in the ground configuration; ξ_2 has the same meaning as ξ_1 but is related to the excited configuration. So, for example, when ξ_1 is equal to zero (or 1), then the spin-orbit interaction in the ground configuration is absent (or equals the normal value used in the preceding sections).

ξ_2 keeping constant and equal to 1, the variation of the Faraday rotation *versus* ξ_1 has been calculated, the results are reported in Table 4 where all other parameters used in the calculation are the same as those used in Section 2. In the same table, the data in parentheses are obtained with ξ_2 being 0. From the table, two important points should be immediately noted: (1) when there is no spin-orbit interaction of the ground configuration, the Faraday rotation almost does not exist; (2) the spin-orbit interaction of the excited configuration has only a very small influence on the Faraday rotation whatever the ξ_1 value is. It should

Table 4. The variation of the full Faraday rotation (in degr cm$^{-1}/x$) at 300 K produced by the Ni^{2+} ions in $Ba_{1-x}M_xFe_{12-x}Ni_xO_{19}$ assuming that all of them are distributed over the 2*b* sites *versus* ξ_1, ξ_2 being equal to 1. The data given in parentheses are the corresponding values when ξ_2 is taken to be 0.

Photon energy (eV)	1	2	2.5	4	6
$\xi_1 = 0$	−11	−48	−77	−231	−737
	(−0)	(−0)	(−0)	(−0.01)	(−0.04)
$\xi_1 = 0.01$	−4	−18	−31	−108	−441
$\xi_1 = 0.25$	1520	6140	9665	25 551	61 478
	(1531)	(6184)	(9736)	(25 765)	(62 168)
$\xi_1 = 0.50$	2344	9474	14 918	39 514	95 537
	(2282)	(9218)	(14 513)	(38 412)	(92 729)
$\xi_1 = 1$	2399	9692	15 256	40 351	97 220
	(2406)	(9940)	(15 304)	(40 497)	(97 220)
$\xi_1 = 2$	2844	10 945	14 559	53 296	128 277
	(2441)	(9864)	(15 529)	(41 101)	(99 236)
$\xi_1 = 4$	2759	10 726	15 767	55 024	128 382
	(2460)	(9940)	(15 650)	(41 422)	(100 067)

Table 5. The variation of the full Faraday rotation *versus* ξ_2, ξ_1 being equal to 1. The data given in parentheses are the corresponding values when ξ_1 is taken to be zero. Other conditions are the same as Table 4.

Photon energy (eV)	1	2	2.5	4	6
$\xi_2 = 0$	2406	9721	15 304	40 500	97 720
	(−0)	(−0.003)	(−0.005)	(−0.01)	(−0.03)
$\xi_2 = 0.25$	2404	9713	15 292	40 461	97 597
	(−2.9)	(−11.9)	(−19.3)	(−57.8)	(−185)
$\xi_2 = 0.50$	2403	9706	15 280	40 424	97 472
	(−5.7)	(−23.9)	(−38.6)	(−115)	(−369)
$\xi_2 = 1$	2399	9691	15 256	40 351	97 220
	(−11.4)	(−47.6)	(−77.1)	(−231)	(−737)
$\xi_2 = 2$	2392	9662	15 208	40 200	96 700
	(−22.7)	(−95.2)	(−154)	(−460)	(−838)
$\xi_2 = 4$	2378	9600	15 106	39 883	95 595
	(−45.4)	(−190)	(−307)	(−919)	(−2940)

be noted that these two points are valid in a large photon energy range (1 ∼ 6 eV) for ξ_1 varying from 0 to 4.

We present in Table 5 the data obtained with ξ_2 varying now from 0 to 4, ξ_1 being equal to 1 or 0 (in this latter case, the Faraday rotation values are given in parentheses). It can be seen that the influence of ξ_2 on the Faraday rotation is small, when ξ_1 is equal to 1. When ξ_1 is equal to zero, the Faraday rotations scale almost linearly with ξ_2. However, it should be noted that in the last case the Faraday rotations are very small.

From these two tables, we arrive at the following conclusions. (i) The spin-orbit interaction of the ground configuration is needed to produce a large Faraday rotation; if there is not so, the Faraday rotation will become very small. However, although the Faraday rotations increase rapidly in the $0 \sim 0.25\ \xi_1$ range, the Faraday rotations approach saturation when ξ_1 reaches 0.5 and then vary very slowly with ξ_1. (ii) Contrarily to the widely spread idea [24,28], the spin-orbit interaction of the excited configuration has almost no effect on the MO effects. In order to reveal the underlying physical origin of the above results, the energies, occupation probabilities, and $\sum_n B_{ng}$ associated with various even-parity-CF-SO and superexchange-interaction split $3d^8$ states are useful tools. $\sum_n B_{ng}$ are the sum of all the matrix elements associated with the transitions from a $3d^8$ state $|g\rangle$ to various $3d^7 4p$ states.

Now, we return to Figure 1, obtained when the spin-orbit coupling of the ground configuration is taken to be the actual value (*i.e.* $\xi_1 = 1$). In this case, all the lowest three even-parity-CF and SO split $3d^8$ levels are doubly degenerate. Their degeneracy is lifted by the superexchange interaction. When ξ_1 becomes 0.25, the energy gaps between these three levels become smaller and the second level cannot be split by the superexchange interaction (see Fig. 7a). The wave function of the state $|g_1\rangle$ (Fig. 7a) is close to the corresponding one of the state $|g_1\rangle$ obtained when $\xi_1 = 1$ (Fig. 1). Similarly, the wave functions of the states $|g_2\rangle,\ \ldots|g_6\rangle$ are close to the corresponding ones of $|g_2\rangle,\ \ldots|g_6\rangle$ in Figure 1. When the spin-orbit coupling of the ground configuration is absent ($\xi_1 = 0$), the lowest even-parity-CF split level is six-fold degenerate, and it is split into 3 doublets by the superexchange interaction as shown in Figure 7b. Being similar to the case of $\xi_1 = 0.25$, now the wave functions of the states $|g_1\rangle,\ \ldots|g_6\rangle$ are also close to the corresponding ones of $|g_1\rangle,\ \ldots|g_6\rangle$ in Figure 1. Now, the energy gap between this and the second CF split level is so large that the contribution of the latter to the Faraday rotation is negligible. In Figures 1, 7a, and 7b the values of $\sum_n B_{ng}$ related to various $3d^8$ states are given. It should be noted that all these values were obtained with $\xi_2 = 1$ (*i.e.* the spin-orbit coupling of the excited configuration was taken to be the actual value).

From Figures 1 and 7, the following points can be noticed. (1) The energy schema in the case of ξ_1 being 0.25 is similar to that obtained with ξ_1 being 1. However, as the spin-orbit coupling strength decreases, the mixing of different ground term (^3F) multiplets by the crystal field becomes stronger and consequently the energy gaps between the lowest three CF-SO split levels decreases. When $\xi_1 = 0$, the lowest CF split level becomes six-fold degenerate. (2) In the cases of $\xi_1 = 1$ and 0.25, the values of $\sum_n B_{ng}$ associated with the two superexchange-interaction split sublevels of any one of the three CF-SO split levels have the same magnitude and are of opposite sign. Therefore the Faraday rotation comes from the differences of the occupation probabilities of the two sublevels

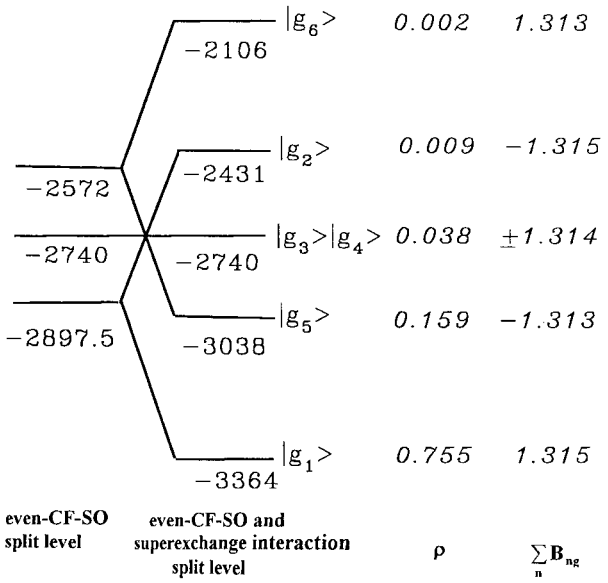

(a)

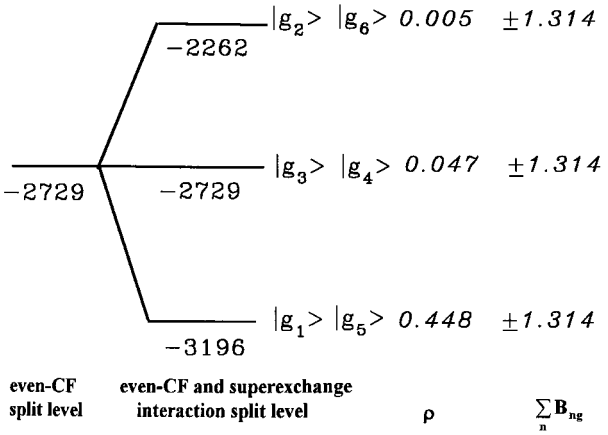

(b)

Fig. 7. Same as Figure 1 but for $\xi_1 = 0.25$ (a), and $\xi_1 = 0$ (b); in the latter case, there are only 3 levels.

of the three doublets. However, when ξ_1 is 1, the occupation probabilities of the second and third CF-SO split levels (located at -2903 and -2195 cm^{-1}, respectively) are so small that only the two sublevels of the lowest one (at -3456 cm^{-1}) contribute to the Faraday rotation. When ξ_1 is equal to 0.25, we also have to pay attention to the second and third CF-SO split $3d^8$ levels. Firstly, the difference of the occupation probabilities of the two sublevels ($|g_1\rangle$ and $|g_2\rangle$) of the lowest CF-SO split level is now equal to 0.746 (Fig. 7a) which is less than the corresponding value (0.959) obtained with ξ_1 being 1 (Fig. 1). Secondly, the difference of the occupation probabilities of the two sublevels ($|g_5\rangle$ and $|g_6\rangle$) of the third CF-SO split level (located at -2572 cm^{-1}) now equals 0.157 and the sign of the quantity $\sum_n B_{ng}$ associated with the low-lying sublevel of this CF-SO split level is opposite to that corresponding to the low-lying sublevel of the lowest CF-SO split level (at -2897.5 cm^{-1}). Consequently, the Faraday rotations contributed by the third and the lowest CF-SO split levels are of opposite sign. As shown in Figure 7a, the degeneracy of the second CF-SO split level (at -2740 cm^{-1}) is not lifted by the superexchange interaction. The values of $\sum_n B_{ng}$ associated with the two orthogonal states of this degenerate level have the same magnitude and are of opposite sign. So this level does not contribute to the Faraday rotation. Finally, the magnitude of the calculated Faraday rotation with $\xi_1 = 0.25$ is smaller than that obtained with $\xi_1 = 1$. (3) In the case of $\xi_1 = 0$, the quantities of $\sum_n B_{ng}$ associated with the two orthogonal states of each of the 3 doublets of the lowest even-parity-CF split $3d^8$ level have the same magnitude and are of opposite sign. Therefore the $3d$ doublets have no net contribution to the Faraday rotation. As a result, the magnitude of the Faraday rotation decreases rapidly as ξ_1 decreases from 0.25 to 0 and approaches zero as reaches zero. When ξ_1 equals 0.5, the occupation probability of the lowest CF-SO and superexchange-interaction split level is 0.91 (it is only a bit less than the corresponding value obtained with ξ_1 being 1); therefore the Faraday rotations almost reach saturation. The values of the Faraday rotation vary very slowly as the spin-orbit interaction strength increases further.

The spin-orbit interaction of the excited configuration only changes the splitting of the $3d^7 4p$ states. But the magnitude of such a change is much less than the difference between the average energies of the excited and ground configurations. This fact explains why the spin-orbit interaction of the excited configuration has only a very small influence on the Faraday rotation below 6 eV photon energy. It should be noted that in all the calculations in this section, all other parameters (crystal field, exchange field, $\langle r \rangle_{3d4p}$, etc.) are the same as those used in the preceding sections, only the spin-orbit coupling strengths are supposed to be variables. The Zeeman effect of the excited configuration has been considered, so the calculated results given in Tables 4 and 5 are full Faraday rotations.

We would like to recall that in the photon energy range of $1 \sim 6$ eV, the diamagnetic Faraday rotation is very small compared with the paramagnetic one (Tab. 2). So, from Tables 4 and 5, it is not able to judge if the spin-orbit interaction is needed to produce the diamagnetic Faraday rotation. It needs a special study. The theoretical room temperature diamagnetic $\frac{1}{9}(\bar{n}^2+2)^2 \frac{\pi}{\lambda \bar{n}} \varepsilon''_{xy}$ spectrum obtained with ξ_1 and ξ_2 being 1 and 0, respectively, is shown by the dotted curve in Figure 5. By comparing this curve with the solid curve in this figure, it can be concluded that the spin-orbit coupling of the excited configuration is also not needed to produce the diamagnetic Faraday rotation. It only leads to small changes of the diamagnetic Faraday spectrum. The effect of the spin-orbit interaction of the ground configuration on the diamagnetic MO effect has also been studied. The corresponding $\frac{1}{9}(\bar{n}^2+2)^2 \frac{\pi}{\lambda \bar{n}} \varepsilon''_{xy}$ spectra obtained in the case of $\xi_1 = 0$, $\xi_2 = 0$ and in the case of $\xi_1 = 0$, $\xi_2 = 1$ are shown in Figure 8. In the latter case, only the spectrum below 16.2 eV is given. By comparing these two curves with those given in Figure 5, it can

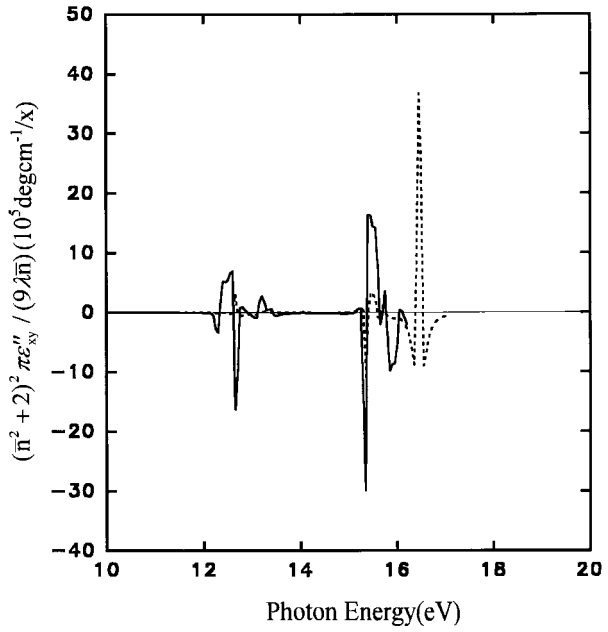

Fig. 8. The room temperature diamagnetic $(\bar{n}^2 + 2)^2\pi\varepsilon''_{xy}/(9\lambda\bar{n})$ spectrum produced by the Ni^{2+} ions in $Ba_{1-x}M_xFe_{12-x}Ni_xO_{19}$ assuming that all of them are distributed over the 2*b* sites. Solid curve obtained when $\xi_1 = 0$, $\xi_2 = 1$, dotted curve obtained when both ξ_1 and ξ_2 are set to zero.

be concluded that the spin-orbit interaction of the ground configuration plays an important role in the diamagnetic MO effect and the diamagnetic MO effect becomes very weak when the relative spin-orbit coupling strength of the ground configuration ξ_1 is set to zero.

At the end of this section, we would like to point out that $\sum_n B_{ng}$ is not a good quantity for determining the Faraday rotation. From equation (4) it can be seen that the Faraday rotation produced by the $|g\rangle \rightarrow |n\rangle$ transition is also determined by the value of the frequency factor. So, $\sum_n B_{ng}$ is, strictly speaking, of less meaning. However it is too tedious to list a lot of B_{ng} values. Therefore only some of the values of $\sum_n B_{ng}$ are given to show the main features. In our calculations, the frequency factor has been considered rigorously.

5 Conclusions

From the above calculations, the following main conclusions are derived. (1) The intra-ionic electric dipole transition from the $3d^8$ to $3d^7 4p$ configurations is important in the origin of the giant MO enhancement of the Ni^{2+} ions in barium ferrites. (2) The intra-ionic $d \rightarrow d$ electric dipole transition induced by the odd-parity crystal field does produce Faraday rotation resonance peaks in the visible range but the magnitude is too small to explain the observed Faraday rotation. (3) The most important factor in the occurrence of the Faraday rotation is the exchange interaction. If there is no Zeeman effect, there will be no Faraday effect. Since the superexchange interaction between the Ni^{2+} and Fe^{3+} ions in the barium ferrite is strong, the visible range Faraday rotation produced by the Ni^{2+} ions is large though that the energy difference between the $3d^8$ and $3d^7 4p$ configurations is large. (4) If only the Zeeman effect of the ground configuration is taken into account while the Zeeman effect of the excited configuration is neglected, the paramagnetic type Faraday effect will be obtained. If we consider the Zeeman effect of the excited configuration but neglect that of the ground configuration, the diamagnetic type Faraday effect will be obtained. The full Faraday rotation is obtained when the Zeeman effects of both the ground and excited configurations are considered. The full Faraday rotation contains both components of the para- and dia-magnetic Faraday rotations, but it is mainly determined by the paramagnetic Faraday rotation. (5) The spin-orbit interaction of the ground configuration plays a very important role in the occurrence of the Faraday rotation produced by the Ni^{2+} ions in barium ferrite. If there is no spin-orbit interaction in the ground configuration, there will be nearly no Faraday rotation. However, different from the theoretical results for the transition metals Fe, Ni, Co [26] and MnBi [25], the Faraday rotation does not increase linearly with the strength of the spin-orbit coupling. The spin-orbit coupling of the excited configuration has only a very weak effect on the Faraday rotation; it is not needed to produce the Faraday rotation. (6) The mixing of different multiplets of the ground term led by the crystal field has a great influence on the MO properties and cannot be neglected. Consequently, the exchange field rather than the molecular field should be used to take the exchange interaction into account.

This work has been partly supported by the National Natural Science Foundation of China (NSFC), NSF of the Education Commission of Jiangsu Province of China and realized in the frame of an official collaboration between the NSFC and the Centre National de la Recherche Scientifique of France.

References

1. M. Naoe, S. Hasunuma, Y. Hoshi, S. Yamanaka, IEEE Trans. Magn. **17**, 3184 (1981).
2. M. Matsumoto, A. Morisaho, T. Haeiwa, K. Naruse, T. Karasawa, IEEE Translat. J. Magn. Jpn **6**, 648 (1991).
3. H. Machida, F. Ohmi, Y. Sawadw, Y. Kaneko, A. Watada, H. Nakamura, J. Magn. Magn. Mater. **54-57**, 1399 (1986).
4. E. Lacroix, P. Gerard, D. Challeton, B. Rolland, B. Becheret, J. Phys. Colloq. France **49**, C8-941 (1988).
5. R. Atkinson, R. Gerber, P. Papakonstantinou, I.W. Salter, Z. Simsa, J. Magn. Magn. Mater. **104-107**, 1005 (1992).
6. Z. Simsa, P. Gornet, A.J. Pointon, R. Gerber, IEEE Trans. Magn. **Mag-26**, 2789 (1990).
7. Z. Simsa, J. Kolacck, J. Simsova, P. Gornet, K. Fisher, R. Gerber, J. Magn. Magn. Mater. **104-107**, 403 (1992).
8. H. Nakamuda, F. Ohmi, Y. Kaneko, Y. Sawada, A. Watada, H. Machida, J. Appl. Phys. **61**, 3346 (1987).
9. M. Gomi, K. Shimai, J. Cho, M. Abe, J. Appl. Phys **73**, 6145 (1993).

10. R. Carey, P.A. Gago-Sandoval, D.M. Newman, B.W.J. Thomas, J. Appl. Phys. **75**, 6789 (1994).
11. M. Abe, M. Gomi, J. Appl. Phys. **53**, 8172 (1982).
12. K. Shinagawa, K. Tamanoi, T. Saito, Y. Aman, K. Sato, T. Tsushima, J. Phys. Colloq. France **49**, C8-959 (1988).
13. R.K. Ahrenkiel, S.L. Lyn, T.J. Coburn, J. Appl. Phys. **46**, 894 (1975).
14. Y. Xu, M. Duan, Phys. Rev. B **46**, 11636 (1992).
15. J.H. Yang, Y. Xu, G.Y. Zhang, J. Appl. Phys. **75**, 6798 (1994).
16. J.H. Yang, Y. Xu, F. Zhang, M. Guillot, Phys. Rev. B **56**, 11119 (1997).
17. Y.R. Shen, Phys. Rev. **133**, A511 (1964).
18. W.A. Crossley, R.W. Cooper, J.L. Page, R.P. van Stapele, Phys. Rev. **181**, 896 (1969).
19. R. Atkinson, R. Gerber, P. Papakonstantinon, I.W. Slater, Z. Simsa, J. Magn. Magn. Mater. **104-107**, 1005 (1992).
20. Y. Xu, G.L. Yang, D.P. Chu, H.R. Zhai, J. Magn. Magn. Mater. **31-34**, 815 (1983).
21. Y. Xu, G.L. Yang, H. Cai, H.R. Zhai, IEEE Trans. Magn. **Mag-20**, 1227 (1984).
22. M. Guillot, H. Le Gall, J. Phys. France **38**, 871 (1977).
23. C.E. Moore, Atomic Energy Levels (Natl. Stand. Ref. Data Ser. 35/VI Nat. Bur Stand. 1971).
24. H.R. Hulme, Proc. R. Soc. Lond. A **135**, 237 (1932).
25. D.K. Misemer, J. Magn. Magn. Mater. **72**, 267 (1988).
26. P.M. Oppenear, J. Sticht, T. Maurer, J. Kiibler, Z. Phys. B **88**, 309 (1992).
27. G.F. Dionne, G.A. Allen, J. Appl. Phys. **75**, 6372 (1994).
28. G.F. Dionne, G.A. Allen, J. Appl. Phys. **73**, 6127 (1993).